Ethanol-Promoted High-Yield Growth of Few-Walled Carbon Nanotubes

Yongyi Zhang,[†] John M. Gregoire,[‡] R. B. van Dover,[‡] and A. John Hart*[,†]

Mechanosynthesis Group, Department of Mechanical Engineering, University of Michigan, 2350 Hayward Street, Ann Arbor, Michigan 48109, Department of Materials Science and Engineering and Cornell Fuel Cell Institute, Cornell University, Ithaca, New York 14853

Received: January 13, 2010; Revised Manuscript Received: March 9, 2010

We report the use of a small concentration of ethanol in addition to ethylene as the carbon source for growth of dense vertically aligned "forests" of few-walled carbon nanotubes (CNTs). Through a detailed comparison of CNTs grown with and without ethanol added to the C_2H_4/H_2 feedstock, we quantify several important effects of the ethanol addition. We show that ethanol selectively reduces the number of CNT walls without changing the outer diameter, increases the catalyst lifetime more than 3-fold, and increases the rate of carbon conversion more than 5-fold. Online dewpoint and mass spectrometry measurements of the exhaust stream suggest that ethanol decomposes into active carbon species that enhance growth, and into H_2O, which counteracts the accumulation of amorphous carbon and thus prolongs the catalyst lifetime. We performed a systematic study of the effect of the catalyst film thickness, and identify a set of conditions that provides growth of millimeter-tall double-walled CNT forests. Importantly, our study reveals that the chemistry of the CVD atmosphere alone plays a critical role in controlling the structure of CNTs, and that addition of ethanol results in few-walled CNTs over a broad range of growth conditions. These findings are an important step toward the ultimate goal of control of CNT chirality during synthesis as well as toward realization of important large-scale applications of aligned CNT films having high monodispersity and structural quality.

Introduction

The synthesis of vertically aligned carbon nanotube (CNT) forests has been studied widely, and there have been myriad lab-scale demonstrations of the utility of CNT forests for mechanical, electrical, thermal, fluidic, adhesive, and other applications.[1–7] In spite of this important progress, most commercial applications will demand efficient production of large quantities of CNT forests along with high standards for the purity, diameter, length, density, and structural quality of the CNTs.

In pursuing these goals, a particular challenge of CNT synthesis by chemical vapor deposition (CVD) is to balance competing reaction pathways that lead to desirably high growth rates and the formation of amorphous carbon that undesirably coats the catalyst and the already-grown CNT sidewalls. In addition, high densities of small catalyst particles that are suitable for growing small-diameter (e.g., <5 nm) CNTs are prone to migration and ripening, which can lead to premature growth termination.[8] These phenomena make it difficult to grow vertically aligned few-walled CNTs while simultaneously achieving high yield, high purity, and high quality. Further, while it is well-established that CNT diameter correlates with the size of the catalyst particle,[9,10] it is not fully understood what determines the number of walls of CNTs when the catalyst preparation conditions are not changed. It is likely that a multitude of factors including the chemistry of the CVD atmosphere, which typically comprises a plurality of species[11] due to thermal decomposition in the growth furnace, are important in mediating structural selectivity of CNT growth. Methods that achieve decoupled control of the CNT diameter and wall number could enable studies of new transport properties, and be a step toward ultimate achievement of chirality-controlled synthesis.

Many efforts have been made toward the highly efficient chemical vapor deposition (CVD) growth of CNT forests in recent years,[7,12] and a now widespread approach is to add a small concentration (typically <1000 ppm) of an oxygen-containing additive such as H_2O[13–15] to prevent the accumulation of amorphous carbon on the catalyst and thereby prolong its lifetime. This species is added to the normal CNT growth feed gas, which typically comprises a hydrocarbon such as ethylene (C_2H_4) or acetylene (C_2H_2), hydrogen (H_2), and an inert carrier gas (e.g., He, Ar). Oxygen[16] and air[17] have been used to improve forest growth as well; however, limiting the concentrations of aggressive oxidants is important to prevent undesired etching of the CNTs. More recently, it was shown that many oxygen-containing small molecules including carbon dioxide,[18] acetone, tetrahydrofuran, ethanol, methylbenzoate, and benzoaldehyde can prolong the lifetime of CNT forest growth in combination with C_2H_2 or C_2H_4.[19] The study by Futaba et al. revealed the generality of oxygen-assisted CNT growth, where the oxygen-containing additive removes amorphous carbon from the catalyst surface. However, a detailed comparison of the structural characteristics (e.g., areal density, diameter, number of walls) of CNTs grown with and without oxygen-containing additives has not been presented. Also, before the first demonstration of H_2O-assisted synthesis, it was shown that single-walled CNT forests can be grown directly from low-pressure ethanol vapor alone, without addition of a pure hydrocarbon or hydrogen.[12,20]

While it is clear that complementary actions by carbon, oxygen, and hydrogen are important to maintain efficient CNT growth, the quantitative effects of these species and of specific growth enhancers on the structural characteristics of CNTs have not been explored in detail. Importantly, it has not been shown

* To whom correspondence should be addressed. E-mail: ajohnh@umich.edu.
[†] University of Michigan.
[‡] Cornell University.

10.1021/jp100358j
Published on Web 03/24/2010

that the gas chemistry itself can mediate the structure of CNTs. We report the results of a detailed study of ethanol-assisted growth of CNT forests from C_2H_4/H_2/He atmosphere, and reveal that adding a small concentration of ethanol as a promoter has multiple important effects. Namely, ethanol (1) selectively reduces the number of walls of the CNTs without changing their outer diameter, (2) significantly increases the growth rate of CNTs without requiring a change of the catalyst or annealing conditions, and (3) significantly prolongs the catalyst lifetime. In combination with tuning of the catalyst thickness using a combinatorial gradient technique, we engineered this process to create millimeter-thick CNT forests with a majority of double-walled CNTs (DWNTs)[21] which are especially attractive for field emission,[22,23] membranes,[24] solar cells,[25] and other devices. The mechanism of ethanol-promoted CNT growth was investigated by online dewpoint and mass spectrometry measurements. This investigation suggests that ethanol decomposes into not only a multitude active carbon species that enhances growth, but also H_2O,[26,27] which counteracts the accumulation of amorphous carbon and thus prolongs the catalyst lifetime.

Experimental Methods

Ethanol-Assisted Growth of CNT Forests. Uniform and gradient Fe catalyst films were studied for synthesis of CNT forests using the ethanol-assisted CVD method. For the uniform catalyst film, 10 nm Al_2O_3 and 1 nm Fe were uniformly deposited on 4 in. Si wafers by electron beam evaporation (Denton model SJ-26 electron beam evaporation system, $\sim 2 \times 10^{-6}$ Torr pressure during deposition), which were first coated with a 500−800 nm film of thermally grown SiO_2. Gradient Fe and Al_2O_3 films with monotonic thickness variations of 0.3−2 and 2.5−40 nm across the wafer, respectively, were deposited by gradient sputtering on 3 in. Si wafers, using a custom-built system described elsewhere.[28] Under the CNT growth conditions, the thin Fe films segregate into nm-scale islands, and thus a quoted film thickness is a measure of the quantity of Fe catalyst. CNT forests were grown at atmospheric pressure in a 1 in. quartz tube furnace with a 30 cm heated length (Lindberg/Blue M; Figure S1 in the Supporting Information). For a typical growth experiment, we first flowed 1000 sccm He (99.999%, PurityPlus Specialty Gases) for 10 min while ramping the temperature to 825 °C, then introduced 400 sccm H_2 (99.999%, PurityPlus Specialty Gases) and 100 sccm He for 5 min to anneal the catalyst. Then, CNT growth began when we diverted the 100 sccm He through a bubbler (7166-16 gas washing bottle, Aceglass, Inc.) filled with anhydrous ethanol (99.5+%, Sigma-Aldrich) and maintained at 22−23 °C, and added 100 sccm C_2H_4 (99.99%, Specialty Gases of America) to the H_2 stream. This stream was issued directly into the furnace. Water-assisted growth was also attempted by filling the bubbler with deionized (DI) water or a water/ethanol mixture instead of anhydrous ethanol. The partial pressure of ethanol or the ethanol/water during growth was adjusted by changing the amount of He diverted into the bubbler.

Moisture Measurement and Mass Spectrometry. The moisture content and the chemical species during the growth process were monitored online with an AMT Dewpoint Hygrometer (Alpha Moisture Systems, England) and an Omnistar Mass Spectrometer (Pfeiffer Vacuum, Inc.) connected in parallel to the outlet of the quartz tube.

Electron Microscopy. The morphology of the CNT forests was characterized by scanning electron microscopy (SEM, Philips XL30-FEG) operating at 15 kV. Transmission electron microscopy (TEM) of the CNTs was performed on a JEOL 3011 operating at 300 kV. Specimens for TEM were prepared by dispersing CNTs into DI water, and then placing one drop of the mixture onto carbon-film coated TEM grids (Cu-400HN, Pacific Grid-Tech).

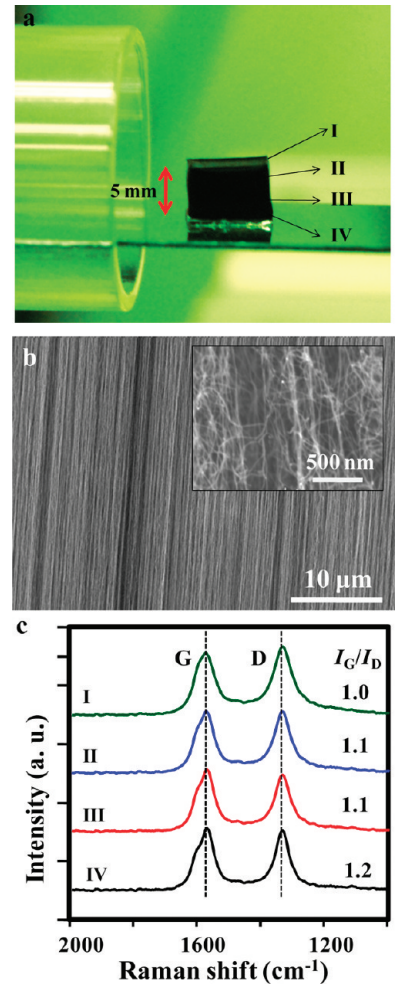

Figure 1. A typical CNT forest grown by the ethanol-assisted method, using 1 nm Fe on 10 nm Al_2O_3, with 6.5 sccm ethanol vapor added to C_2H_4, for a duration of 60 min: (a) photograph of the 5.1 mm high forest resting at the output of the 25 mm diameter quartz furnace tube; (b) SEM images of the typical morphology of the forest sidewall; and (c) Raman spectra (532 nm excitation) taken at the locations indicated in panel a.

Raman Microscopy. Resonance Raman spectra of the CNT forests were taken with a Dimension-P1 Raman system (Lambda Solutions, Inc.) with 532 nm excitation. The laser power is 20 mW and the spot size is ~ 25 μm at 50× magnification.

Thermogravimetric Analysis. Thermogravimetric analysis (TGA) was carried out with a Perkin-Elmer Pyris 1 TGA. The CNT forest was heated from 30 to 950 at 10 deg/min, and held at 950 °C for 10 min, in 20 sccm air flow.

CNT Mass Measurement. The CNT forests were carefully removed from the growth substrates with a razor blade and weighed on a microbalance (Ohaus DV215).

Results and Discussion

Figure 1a shows an optical photograph of a typical CNT forest resulting from 60 min growth time at 825 °C via the ethanol-assisted method. The catalyst here was 1 nm Fe on 10 nm Al_2O_3. The average growth rate of the forest during the 60 min period was 85 μm per minute, and the final height is 5.1 mm. The forest reached 2.6 mm after 20 min, averaging 130 μm per

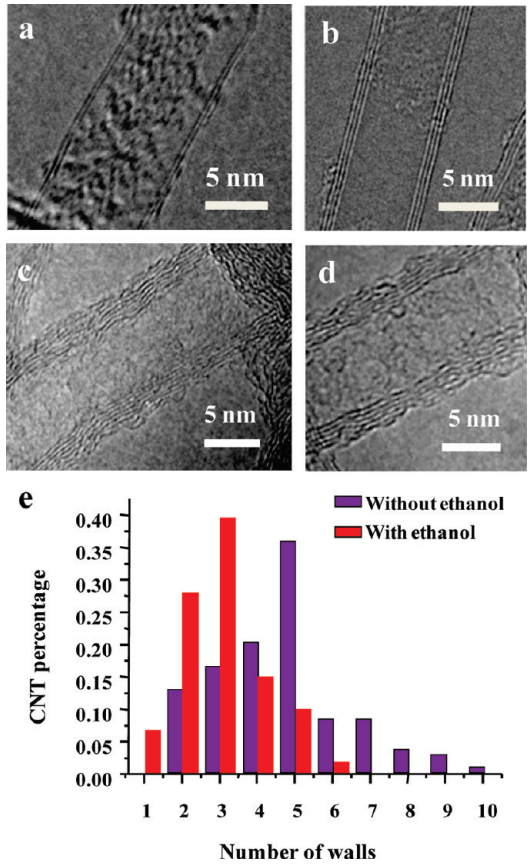

Figure 2. Comparison of CNTs extracted from CNT forests grown with (a, b) and without (c, d) ethanol assistance, demonstrating that ethanol selectively reduces the number of CNT walls, without changing the CNT diameter: (a, b) double- and triple-walled CNTs whose diameters are 9.1 and 6.8 nm; (c, d) multiwalled CNTs with diameters of 10.3 and 10.2 nm. The structural quality of the CNT walls is significantly higher for the sample grown by the ethanol-assisted method. (e) Comparison of the wall number distributions in both cases.

minute. The morphology of the forest sidewall is continuous and uniform from top to bottom, as represented by the SEM images in Figure 1b. Figure 1c shows Raman spectra in the G-band and D-band region of the forest in Figure 1a, where spectra labeled I, II, III, and IV were collected from the top to the bottom of the forest and normalized by the D-band. The peak intensities of the G-band (I_G, 1581 cm^{-1}) and D-band (I_D, 1336 cm^{-1}) regions were determined for each spectrum. From the top to the bottom of the forest, the I_G/I_D ratio gradually increases from 1.0 to 1.2 since the forest adapts a "base-growth" mode[13,29] and the time of exposure to amorphous carbon deposition[17,30] is much longer at the top than that at the bottom. It is important to note here that while a high I_G/I_D ratio is typically measured for single-walled CNTs, this is not expected for larger-diameter few-walled CNTs because of the significant decrease in the resonant Raman enhancement as CNT diameter increases. In this regard, TEM imaging is a more direct measure of the CNT structural quality. Further, TGA (Figure S2 in the Supporting Information) performed in air shows that there is negligible mass loss until the temperature exceeds 700 °C. The absence of mass loss below 500 °C verifies that CNT forests grown by the ethanol-assisted method have high purity, because amorphous carbon typically oxidizes below 500 °C.

Accordingly, Figure 2 shows TEM images of the CNTs grown with and without ethanol assistance, revealing that addition of ethanol to the CVD atmosphere selectively produces

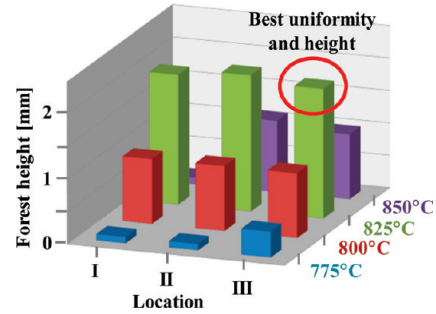

Figure 3. Variation of CNT forest height with furnace control temperature and downstream location within the reactor tube. The locations of I, II, and III are 0, 4, and 8 cm downstream of the center (thermocouple location) of the quartz tube, respectively. All experiments were performed with 15 min of carbon supply. The forest with the best combination of height and uniformity was obtained at 825 °C, at downstream position III.

CNTs with fewer walls, without changing the CNT diameter. With ethanol assistance, the average CNT diameter is approximately 8.1 nm, and the average number of walls is about 3.0 (61 tubes). The majority of the sample is 2−4 walled CNTs with diameters varying from 7 to 9 nm. CNTs grown in an identical recipe without ethanol have an average diameter close to 8.5 nm (139 tubes), and an average of 4.6 walls (109 tubes). These statistics are shown in Figure S3 in the Supporting Information. The TEM images also show that the CNTs grown with ethanol exhibit significantly less amorphous carbon on their sidewalls and have better crystallinity, indicating that the ethanol-assisted process improves both the purity and structural quality of the CNTs within the forests.

Before reaching this operating point, a matrix (Figure 3, as well as Figure S4 in the Supporting Information) of CNT growth experiments with and without added ethanol was performed to optimize the forest height and evaluate the effects of ethanol on the growth kinetics and CNT characteristics. In each experiment, three substrates were loaded at locations I, II, and III which were 0, 4, and 8 cm from the center of the furnace tube (the location of the control thermocouple). At these locations, the temperature was approximately 0, 25, and 50 °C lower than the set point temperature, respectively. For 15 min ethanol-assisted growth experiments at setpoint temperatures of 775, 800, 825, and 850 °C, the forest heights plotted in Figure 3 were achieved. The highest forests were obtained at 825 °C, at location III.

Notably, with 100 sccm He bubbling through ethanol (23 °C), the lifetime of the catalyst was significantly prolonged to exceed 100 min, and the forest reached a terminal height exceeding 5 mm. By comparison, without ethanol assistance the growth stopped after approximately 20 min, resulting in a maximum forest height of approximately 2.5 mm. In both cases, the variation of forest height and growth rate with sample position in the tube furnace was related to the important role of thermal decomposition of the carbon feedstock in determining the production of carbon species that contribute to CNT growth.[11,31]

CNT Forest Mass and Height Kinetics. Figures of merit for average CNT growth kinetics were obtained by measurements of the mass and height of the CNT forest. The mass is a measure of the rate of carbon conversion at the catalyst, and the height is an approximate measure of the rate of CNT lengthening.[32] While the ratio of these quantities provides a carbon density in the forest, more detailed measurements are needed to distinguish possible spatial variations of the number density of CNTs, the average CNT wall number, and the mass of amorphous carbon.

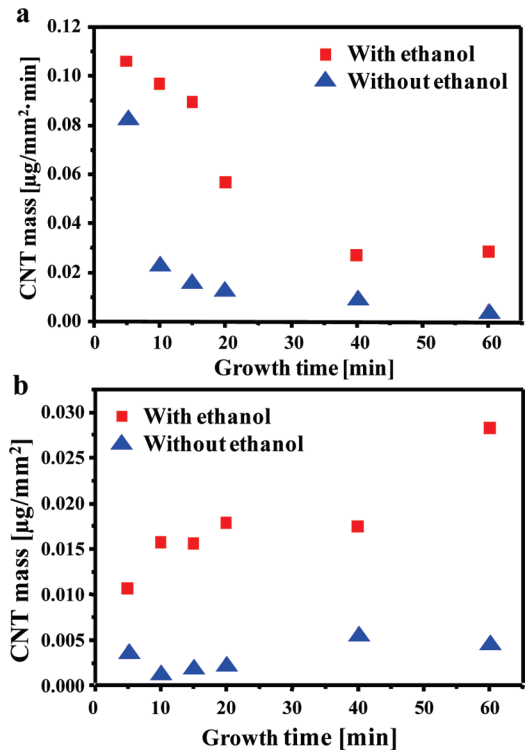

Figure 4. Significant enhancement of CNT yield by addition of ethanol to the CVD atmosphere, quantified in terms of (a) time averaged CNT mass accumulation rate per unit area [μg/(mm^2·min)] and (b) total CNT forest mass per unit area [μg/mm^2] after the specified growth duration.

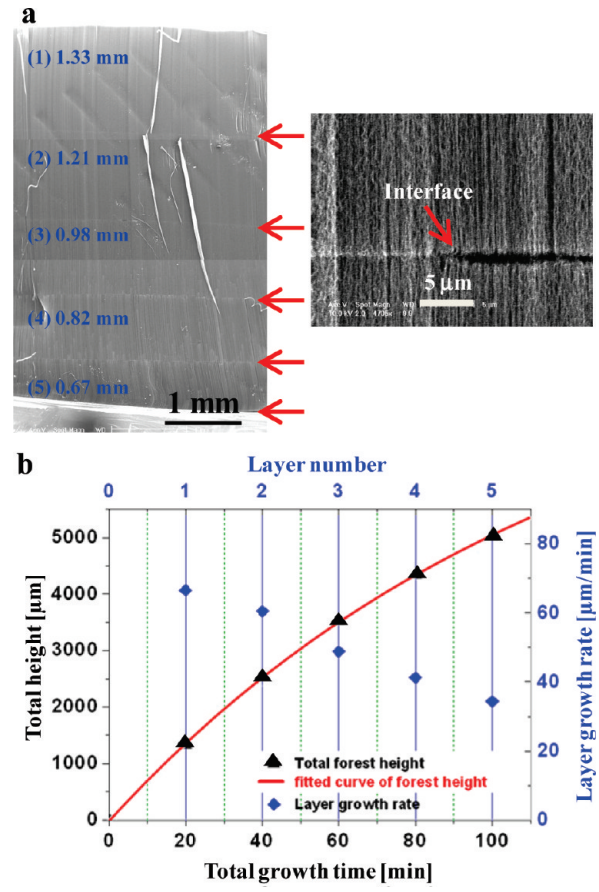

Figure 5. (a) SEM characterization of CNT forest grown by the pulsed method (5 × 20 min) at 825 °C, with text indicating the layer height of each pulse, and a close view of the layer−layer interface. (b) The relationship between forest height h (μm) and growth time t (min) is fitted by $h(t) = \gamma_0\tau[1 - \exp(-t/\tau)]$, where γ_0 is the initial growth rate, and τ is a time constant. For this experiment, $\gamma_0 = 74$ μm/min and $t = 120$ min.

First, we quantified the effect of ethanol addition on the CNT forest mass. The results, plotted in Figure 4, demonstrate that adding ethanol significantly enhances the instantaneous yield [mass/(area·time)] as well as the total yield of CNTs for a given reaction time [mass/area]. Regardless of ethanol content, the instantaneous yield (Figure 4a) decreases with time; however, the values for the ethanol-assisted process remain at least 5-fold higher after 10−20 min of growth. The enhancement in total yield (Figure 4b) increases with growth time because ethanol addition results in an increased catalyst lifetime, and therefore produces CNTs for a longer duration. After 60 min, the total yield of CNTs with ethanol assistance is 0.028 μg/mm^2, which is more than 6 times higher than when ethanol is not added. Because the growth recipe is otherwise identical, these measurements indicate that adding ethanol increases the rate of conversion from the gas-phase precursors to CNTs. Therefore adding ethanol to C_2H_4 significantly increases the chemical and energetic efficiency of the CNT growth process.

Complementary information on the CNT height kinetics was obtained by a pulsed growth technique. Here, we halted the flow of C_2H_4 during the growth cycle, while maintaining the flows of H_2 and He (bubbled through ethanol). This method was previously shown to leave a "growth mark" on the sidewall of the CNT forest, due to etching of the CNTs at the catalyst during the pause.[33] During the pause, the ethanol vapor does not present a sufficient carbon supply to maintain forest growth, thus halting the forest growth. When C_2H_4 was reintroduced, forest growth resumed, and a mark was left behind on the forest sidewall. If the catalyst remained active after n growth/pause cycles, there would be n growth marks and $(n + 1)$ layers.

Accordingly, Figure 5 shows how the CNT forest height increased with time based on the pulsed growth technique. There are 5 layers observed after 4 pulses, and the total growth time was 100 min. From the first to the fifth layer, the layer heights are 1330, 1210, 980, 820, and 670 μm, respectively. The relationship between the total forest height (h, μm) and total growth time (t, min) can be fitted (Figure 5b, red curve) by the equation $h(t) = \gamma_0\tau[1 - \exp(-t/\tau)]$, which was derived by Einarsson et al.,[34] and further discussed by Futaba et al.,[14] and Xiang et al.[27] Here the parameter γ_0 represents the initial growth rate, and τ is a time constant. The fitted values are $\gamma_0 = 74.3$ μm/min and $\tau = 119.9$ min. The ability to reactivate the catalyst after the carbon source has been interrupted also indicates promise to manufacture multiple CNT forests by repeated growth and delamination sequences using the same catalyst layer.[35] This is a useful approach to continuous manufacturing[36] of CNT forests for many applications including toughened composites[37] and nanofiltration membranes.[38]

Production of DWNT Forests by Tuning the Catalyst Film Thickness. Catalyst thin films with a gradient in thickness facilitated a high-throughput study of the relationship between the catalyst film thickness and the CNT diameter and wall number. Similar combinatorial techniques have been applied for SWNT and MWNT growth in past studies.[18,20,39,40] Figure 6a shows thickness distributions of the gradient Fe film and Al_2O_3 film along one edge of the substrate, which was prepared by sputter deposition, as described in the Experimental Methods. From left to right, the Fe catalyst layer and the Al_2O_3 buffer layer thicknesses vary from 0.52 to 0.72 nm and from 33 to 23

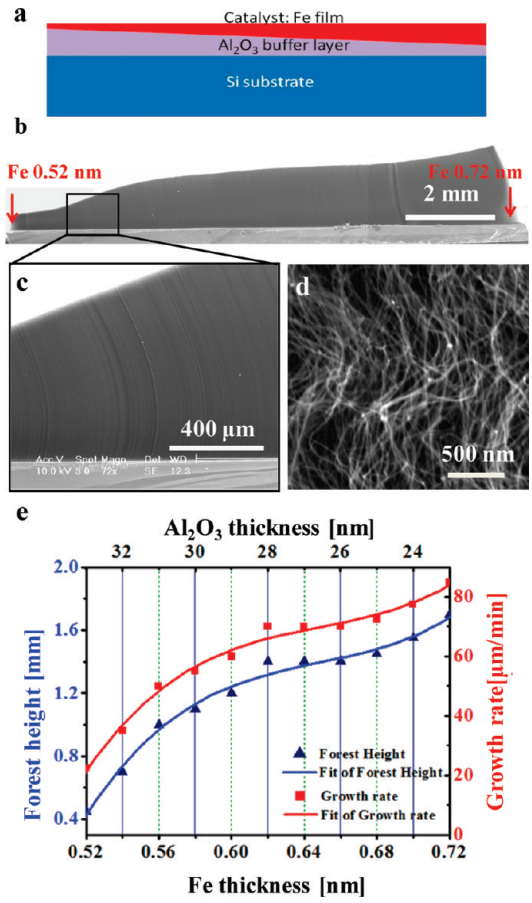

Figure 6. Characterization of ethanol-assisted growth on a spread composition Fe/Al_2O_3 film: (a) diagram of the gradient catalyst film, with Fe thickness ranging from 0.52 to 0.72 nm; (b) SEM images of the forest growth from the gradient film; (c, d) close-up SEM images of the forest, showing mechanical coupling due to the spatial variation of growth rate; and (e) plots of forest height (*h*, blue) and forest growth rate (*r*, red) versus the catalyst thickness mapped across the sample.

nm. Our studies indicate that the variation in Al_2O_3 does not affect CNT growth.

The substrate with gradient films was placed in the growth furnace operated under the ethanol-assisted growth conditions described above. CNT growth occurred simultaneously at all Fe thicknesses. The lateral extent of the gradient film was sufficiently large that the thickness gradient at a given CNT growth site was negligible. The gradient film thickness resulted in a smooth gradient in CNT forest height, as shown in Figure 6b. The spatial variation of the forest growth rate caused mechanical stress in the forest, which drastically bent the CNTs toward the direction where the growth rate was lower. A higher magnification SEM image of the bending CNT forest (Figure 6d) shows that the CNTs grew in a coordinated wave-like fashion. The relationship between Fe thickness and CNT height is shown in Figure 6e; from right to left along the substrate edge diagrammed in Figure 6a, the CNT forest height increased nonlinearly from 0.45 mm on the left to 1.70 mm on the right.

TEM images reveal the effect of Fe thickness on the CNT structure. Small segments of the CNT forest from regions of interest were carefully removed with tweezers and put onto TEM grids for characterization. As shown in Figure S4 in the Supporting Information, the CNTs harvested from the 0.54 nm Fe region have fewer walls and a narrower wall distribution, compared with these from the 0.70 nm Fe region. The majority of CNTs grown from 0.70 nm Fe have 2−5 walls, and the

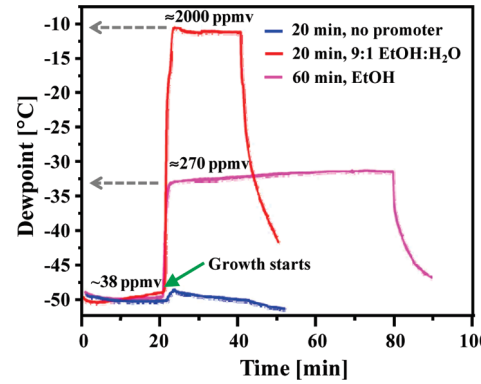

Figure 7. Effect of ethanol and ethanol/water addition (via bubbling of He through the liquid) on the water vapor concentration during CNT growth, measured using a hygrometer placed at the output of the tube furnace. The plot compares (i) a control experiment without added ethanol vapor, giving ~38 ppmv H_2O, (ii) a typical ethanol-assisted CVD with 100 sccm He bubbled through anhydrous ethanol, giving ~270 ppmv H_2O, and (iii) CVD with 100 sccm He bubbled through 9:1 ethanol:water, giving ~2000 ppmv H_2O.

average wall number is 3.0. The average CNT diameters resulting from 0.54 and 0.72 nm Fe are 7.0 and 7.2 nm, respectively (Figure S4 in the Supporting Information), but this difference is within the uncertainty of measurement with TEM imaging. Thus, we observe that the Fe thickness affects the number of CNT walls, but does not affect the CNT outer diameter. This further demonstrates that ethanol promotes growth of CNTs having a relatively small number of walls compared to their diameter.

Role of Ethanol as a CNT Growth Promoter. It is evident that adding a low concentration of ethanol to the C_2H_4/H_2 feedstock increases the CNT growth rate, prolongs the catalyst lifetime, and most importantly promotes growth of few-walled CNTs. This implies that ethanol affects the gas-phase formation of active carbon species in the high-temperature environment, and modifies the gas−catalyst interactions which determine how the CNT is formed.

Further insight on the thermal decomposition of the reaction atmosphere was obtained by online dew point measurement and mass spectroscopy of the furnace output stream. Figure 7 shows measurements of water vapor concentration throughout the CVD process. In a control experiment where no ethanol was added and the tube was evacuated with a roughing pump prior to purging with He, the H_2O concentration was approximately constant at ~40 ppm throughout the purge, ramp, and annealing stages. The only significant transient occurred when H_2O is formed by reaction of C_2H_4 with residual O_2 in the quartz tube. This occurred immediately when C_2H_4 is introduced, and then the H_2O concentration decreased gradually during the growth stage. Notably, the background level of ~40 ppm was comparable to the optimal level of 100 ppm that has been reported for the water-assisted "super growth" of SWNT forests.[13,14] This suggests that a non-negligible concentration of H_2O may be present, and may play a hidden role in CVD methods that do not intentionally introduce an oxidizing agent. Comparatively, when 100 sccm He was bubbled through ethanol according to our optimal conditions, the H_2O concentration rose sharply from the background level to ~270 ppm when C_2H_4 and ethanol were introduced coincidently. This level remained steady throughout the 60 min growth duration. When the bubbler contains 1:9 H_2O:ethanol, the level rose to ~2000 ppm. In this case, no CNT forest was observed on the substrate after 20 min; presumably the high water concentration etches the CNTs and therefore prevents growth.[13,18]

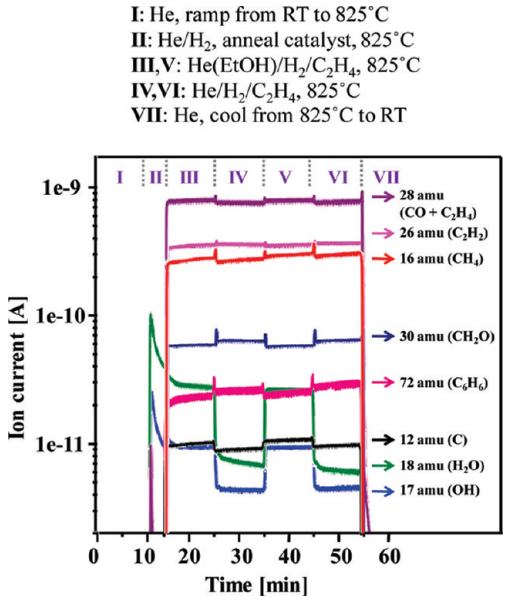

Figure 8. Mass spectra of species measured from the output of the tube furnace during the pulsed CVD process where ethanol is intermittently supplied to the reaction by bubbling through He. The absence of a signal from ethanol (C_2H_5OH, 46 amu) indicates that ethanol thermally decomposes during the CVD process.

At 23 °C and 1 atm of pressure, the saturated vapor pressure of pure ethanol is approximately 6.5 kPa; thus, the bubbling of 100 sccm He through ethanol carried approximately 6.5 sccm ethanol vapor into the system. Comparing the mass flow rates of ethanol (~10 mg/min) and ethylene (~100 mg/min) during the growth period to the mass accumulation rate of CNTs (~0.1 mg cm^{-2} min^{-1}), we conclude that the primary pathway for ethanol decomposition is gas-phase pyrolysis via $C_2H_5OH \rightarrow C_2H_4 + H_2O$.[26] However, the H_2O vapor flow rate corresponding to the measured dewpoint of ~270 ppm is only 0.17 sccm, indicating that the majority of H_2O reacts into other species within the furnace. Further, as we reported in a separate study, C_2H_4 decomposes into a plurality of hydrocarbons due to gas-phase rearrangement in the CVD atmosphere, implying important roles of a variety of species in governing the efficient growth of CNTs.[31,32] Likewise, it is known there are many pathways for ethanol decomposition, which can yield CO, C_2H_2, CH_3CHO, CH_4, and a small amount of CO_2 at elevated temperatures.[26,27]

Figure 8 shows the ion currents of selected species measured throughout the CVD process. Here, the presence of ethanol was toggled on and off twice during the growth stage, facilitating direct comparison of how ethanol affects the chemical composition of the CVD atmosphere. Compared to the periods without ethanol (IV, VI), the ethanol-assisted periods (III, V) gave larger ion currents from C (12 amu), CH_4 (16 amu), OH (17 amu), H_2O (18 amu), and CO/C_2H_4 (28 amu). The large relative increase in H_2O is expected due to pyrolysis of ethanol. The relative contributions of CO and C_2H_4 to the 28 amu signal are unknown; however, it is likely that C_2H_4 dominates. Ethanol has no effect on acetylene (C_2H_2, 26 amu) or benzene (C_6H_6, 72 amu) formation. Further, there was no ion current from ethanol (46 amu) itself, confirming that ethanol was completely decomposed during the process.[27] The absence of a measurable ion current at 44 amu also indicates that no CO_2 was formed. The ion current signal of H_2O gradually decreased during the periods without ethanol, in agreement with the hygrometer measurements. Finally, the increase in the carbon (12 amu) signal suggests there was more highly active carbon during ethanol-assisted growth, which agrees with the enhanced growth rate observed for the ethanol-assisted process.

The large increase in the concentration of the hydroxyl radical (OH) is notable because OH has been shown to maintain catalyst stability by preventing Ostwald ripening of Fe on Al_2O_3.[8] Inhibition of Ostwald ripening is also presumed to be important for growing small-diameter CNTs. In the present study the presence of OH may increase the catalyst lifetime by impeding ripening, and increase the yield through creating a higher density of small catalyst particles. However, the relative invariance of CNT outer diameter with respect to ethanol addition and Fe film thickness suggests that a more complex mechanism determines the number of CNT walls.

Conclusion

We have shown that adding a small concentration of ethanol to a conventional CNT growth process can facilitate control of the number of walls while increasing the CNT yield and prolonging the catalyst lifetime. In particular, adding ethanol to a $C_2H_4/H_2/He$ atmosphere facilitated rapid growth of dense few-walled CNT forests to heights exceeding 5 mm. Further study of the detailed decomposition pathways of hydrocarbon precursors and oxygen-containing additives will give important insights on how the chemistry of the precursor can affect the atomic-scale processes of CNT growth.

Acknowledgment. This work was supported by the National Science Foundation (CMMI-0800213); Airbus S.A.S., Boeing, Embraer, Lockheed Martin, Saab AB, Spirit AeroSystems, Textron Inc., Composite Systems Technology, and TohoTenax through MIT's Nano-Engineered Composite aerospace STructures (NECST) Consortium; and the University of Michigan Department of Mechanical Engineering and College of Engineering. Microscopy and microfabrication were performed at the University of Michigan Electron Microbeam Analysis Library (EMAL) and the Lurie Nanofabrication Facility (LNF), respectively. J. M. Gregoire and R. B. van Dover made use of the facilities of the Cornell Center for Materials Science, which are supported by National Science Foundation award DMR-0520404. We thank Jian Zhu and Jinjing Li for assistance with the TGA experiment, and Prof. Nicholas Kotov for graciously sharing his TGA instrument.

Supporting Information Available: Apparatus for ethanol-assisted growth of CNT forests and optical image forests grown at different positions in the furnace (Figure S1), TGA measurement of CNT forest grown with ethanol assistance (Figure S2), diameter and wall number statistics of the CNTs grown with and without ethanol (Figure S3), optical images of CNT forests grown at different temperatures (Figure S4), and diameter and wall number statistics of CNTs from 0.54 and 0.70 nm Fe regions of spread composition film (Figure S5). This material is available free of charge via the Internet at http://pubs.acs.org.

References and Notes

(1) Chattopadhyay, D.; Galeska, I.; Papadimitrakopoulos, F. *J. Am. Chem. Soc.* **2001**, *123* (38), 9451–9452.
(2) Hinds, B. J.; Chopra, N.; Rantell, T.; Andrews, R.; Gavalas, V.; Bachas, L. G. *Science* **2004**, *303* (5654), 62–65.
(3) Yildirim, T.; Ciraci, S., *Phys. Rev. Lett.* **2005**, *94* (17), 175501.
(4) Yang, L.; Fishbine, B. H.; Migliori, A.; Pratt, L. R. *J. Am. Chem. Soc.* **2009**, *131* (34), 12373–12376.
(5) Qu, L. T.; Dai, L. M.; Stone, M.; Xia, Z. H.; Wang, Z. L. *Science* **2008**, *322* (5899), 238–242.
(6) Jiang, K. L.; Li, Q. Q.; Fan, S. S. *Nature* **2002**, *419* (6909), 801–801.

(7) Fan, S. S.; Chapline, M. G.; Franklin, N. R.; Tombler, T. W.; Cassell, A. M.; Dai, H. J. *Science* **1999**, *283* (5401), 512–514.
(8) Amama, P. B.; Pint, C. L.; McJilton, L.; Kim, S. M.; Stach, E. A.; Murray, P. T.; Hauge, R. H.; Maruyama, B. *Nano Lett.* **2009**, *9* (1), 44–49.
(9) Yamada, T.; Namai, T.; Hata, K.; Futaba, D. N.; Mizuno, K.; Fan, J.; Yudasaka, M.; Yumura, M.; Iijima, S. *Nat. Nanotechnol.* **2006**, *1* (2), 131–136.
(10) Kukovitsky, E. F.; L'Vov, S. G.; Sainov, N. A.; Shustov, V. A.; Chernozatonskii, L. A. *Chem. Phys. Lett.* **2002**, *355* (5−6), 497–503.
(11) Plata, D. L.; Hart, A. J.; Reddy, C. M.; Gschwend, P. M. *Environ. Sci. Technol.* **2009**, *43* (21), 8367–8373.
(12) Maruyama, S.; Einarsson, E.; Murakami, Y.; Edamura, T. *Chem. Phys. Lett.* **2005**, *403* (4−6), 320–323.
(13) Hata, K.; Futaba, D. N.; Mizuno, K.; Namai, T.; Yumura, M.; Iijima, S. *Science* **2004**, *306* (5700), 1362–1364.
(14) Futaba, D. N.; Hata, K.; Yamada, T.; Mizuno, K.; Yumura, M.; Iijima, S., *Phys. Rev. Lett.* **2005**, *95* (5), 056104.
(15) Futaba, D. N.; Hata, K.; Namai, T.; Yamada, T.; Mizuno, K.; Hayamizu, Y.; Yumura, M.; Iijima, S. *J. Phys. Chem. B* **2006**, *110* (15), 8035–8038.
(16) Zhang, G. Y.; Mann, D.; Zhang, L.; Javey, A.; Li, Y. M.; Yenilmez, E.; Wang, Q.; McVittie, J. P.; Nishi, Y.; Gibbons, J.; Dai, H. J. *Proc. Natl. Acad. Sci. U.S.A.* **2005**, *102* (45), 16141–16145.
(17) Li, X. S.; Zhang, X. F.; Ci, L. J.; Shah, R.; Wolfe, C.; Kar, S.; Talapatra, S.; Ajayan, P. M., *Nanotechnology* **2008**, *19* (45), 455609.
(18) Pint, C. L.; Pheasant, S. T.; Parra-Vasquez, A. N. G.; Horton, C.; Xu, Y. Q.; Hauge, R. H. *J. Phys. Chem. C* **2009**, *113* (10), 4125–4133.
(19) Futaba, D. N.; Goto, J.; Yasuda, S.; Yamada, T.; Yumura, M.; Hata, K. *Adv. Mater.* **2009**, *21* (47), 4811–4815.
(20) Sugime, H.; Noda, S.; Maruyama, S.; Yamaguchi, Y. *Carbon* **2009**, *47* (1), 234–241.
(21) Pfeiffer, R.; Pichler, T.; Kim, Y. A.; Kuzmany, H. Double-wall carbon nanotubes. In *Carbon Nanotubes;* Springer: Berlin/Heidelberg, 2008; Vol. 111, pp 495−530.
(22) Son, Y. W.; Oh, S.; Ihm, J.; Han, S. *Nanotechnology* **2005**, *16* (1), 125–128.
(23) Chen, G. H.; Shin, D. H.; Iwasaki, T.; Kawarada, H.; Lee, C. J., *Nanotechnology* **2008**, *19* (41), 415703.
(24) Holt, J. K.; Park, H. G.; Wang, Y. M.; Stadermann, M.; Artyukhin, A. B.; Grigoropoulos, C. P.; Noy, A.; Bakajin, O. *Science* **2006**, *312* (5776), 1034–1037.
(25) Wei, J. Q.; Jia, Y.; Shu, Q. K.; Gu, Z. Y.; Wang, K. L.; Zhuang, D. M.; Zhang, G.; Wang, Z. C.; Luo, J. B.; Cao, A. Y.; Wu, D. H. *Nano Lett.* **2007**, *7* (8), 2317–2321.
(26) Li, J.; Kazakov, A.; Dryer, F. L. *J. Phys. Chem. A* **2004**, *108* (38), 7671–7680.
(27) Xiang, R.; Einarsson, E.; Okawa, J.; Miyauchi, Y.; Maruyama, S. *J. Phys. Chem. C* **2009**, *113* (18), 7511–7515.
(28) Gregoire, J. M.; van Dover, R. B.; Jin, J.; DiSalvo, F. J.; Abruna, H. D., *Rev. Sci. Instrum.* **2007**, *78* (7), 072212.
(29) Li, X. S.; Cao, A. Y.; Jung, Y. J.; Vajtai, R.; Ajayan, P. M. *Nano Lett.* **2005**, *5* (10), 1997–2000.
(30) Yasuda, S.; Hiraoka, T.; Futaba, D. N.; Yamada, T.; Yumura, M.; Hata, K. *Nano Lett.* **2009**, *9* (2), 769–773.
(31) Meshot, E. R.; Plata, D. L.; Tawfick, S.; Zhang, Y. Y.; Verploegen, E. A.; Hart, A. J. *ACS Nano* **2009**, *3* (9), 2477–2486.
(32) Bedewy, M.; Meshot, E. R.; Guo, H.; Verploegen, E. A.; Lu, W.; Hart, A. J. Collective mechanism for the evolution and self-termination of vertically aligned carbon nanotube growth. *J. Phys. Chem. C* **2009**, *113*, 20576−20582.
(33) Liu, K.; Jiang, K. L.; Feng, C.; Chen, Z.; Fan, S. S. *Carbon* **2005**, *43* (14), 2850–2856.
(34) Einarsson, E.; Murakami, Y.; Kadowaki, M.; Maruyama, S. *Carbon* **2008**, *46* (6), 923–930.
(35) Pint, C. L.; Nicholas, N.; Duque, J. G.; Parra-Vasquez, A. N. G.; Pasquali, M.; Hauge, R. *Chem. Mater.* **2009**, *21* (8), 1550–1556.
(36) Polsen, E. S.; Perkins, S. M.; Meshot, E. R.; Bedewy, M.; Figueredo, S.; Steiner, S. A.; Wardle, B. L.; Hart, A. J. Continuous manufacturing of aligned carbon nanotubes for tough and multifunctional interface layers. In *International Conference on Composite Materials*; The British Composites Society: Edinburgh, UK, 2009.
(37) Garcia, E. J.; Wardle, B. L.; Hart, A. J. *Composites, Part A* **2008**, *39* (6), 1065–1070.
(38) Fornasiero, F.; Park, H. G.; Holt, J. K.; Stadermann, M.; Grigoropoulos, C. P.; Noy, A.; Bakajin, O. *Proc. Natl. Acad. Sci. U.S.A.* **2008**, *105* (45), 17250–17255.
(39) Christen, H. M.; Puretzky, A. A.; Cui, H.; Belay, K.; Fleming, P. H.; Geohegan, D. B.; Lowndes, D. H. *Nano Lett.* **2004**, *4* (10), 1939–1942.
(40) Noda, S.; Sugime, H.; Osawa, T.; Tsuji, Y.; Chiashi, S.; Murakami, Y.; Maruyama, S. *Carbon* **2006**, *44* (8), 1414–1419.

JP100358J

Supporting Information for

Ethanol-Promoted High-Yield Growth of Few-Walled Carbon Nanotubes

Yongyi Zhang,† John M. Gregoire,‡ R. B. van Dover,‡ and A. John Hart*,†

Department of Mechanical Engineering, University of Michigan, 2350 Hayward Street, Ann Arbor, Michigan 48109;

Department of Materials Science and Engineering, Cornell University, Ithaca, New York 14853 and Cornell Fuel Cell Institute, Cornell University, Ithaca, New York 14853

Deposition and thickness calibration of gradient catalyst films

We synthesized Fe films with smoothly varying thickness on the sub-nm scale by using a gradient sputtering technique [1]. The thickness profiles for the Fe and Al_2O_3 gradient films were measured in the deposition chamber using a quartz crystal monitor. A direct measure of the profile of deposition rate for each source was obtained by incrementally moving the deposition monitor across the deposition region (in the substrate plane). The calibration films were not deposited during these measurements, but were deposited using the same deposition conditions. This technique for deposition profiling is described in further detail in [1] and is shown to provide robust measurements of film thickness and composition in [1] and [2]. For the Fe thickness profile, the uncertainty in the absolute thickness is 10%. The thickness gradient is guaranteed to be monotonic, and the uncertainty in the relative thickness along the composition gradient is <5%.

The deposition rate measurements are of the *mass* accumulation and have been converted to thickness assuming bulk Fe density. Under the CNT growth conditions, the thin Fe films are known to segregate into nm-scale islands, and thus the quoted Fe thickness is a convenient measure of the quantity of Fe catalyst.

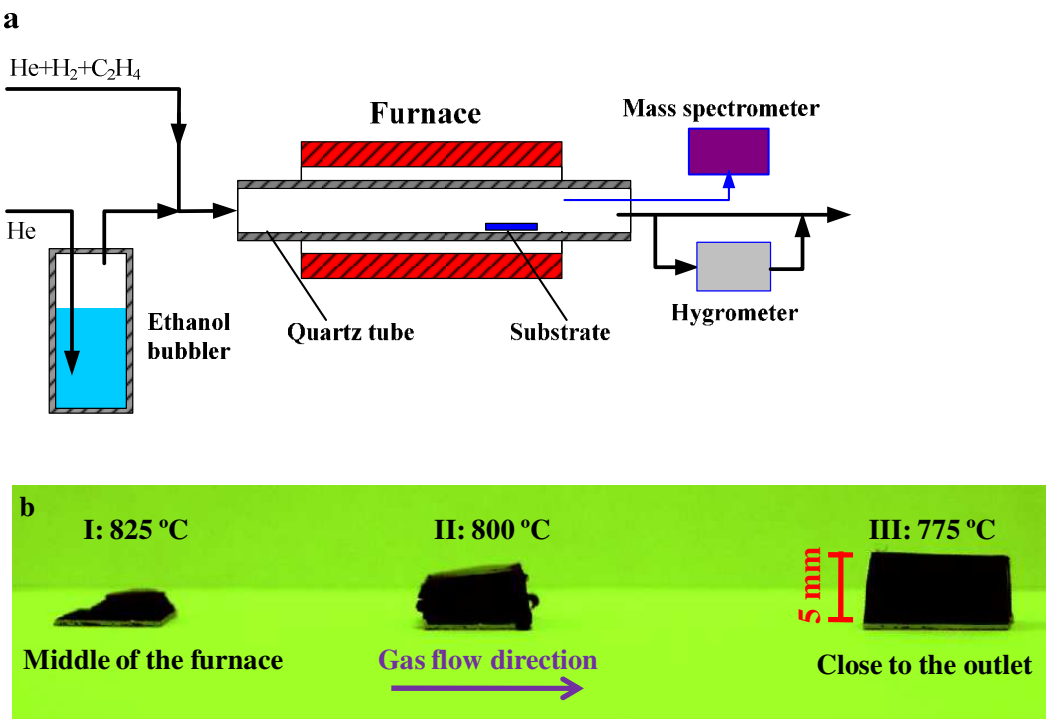

Figure S1. (a) Schematic of apparatus for ethanol-assisted growth of CNT forests, where ethanol is introduced by bubbling He through ethanol. A mass spectrometer and hygrometer are connected to the outlet of the system. (b) CNT forests grown at different locations in the furnace in a 60 min ethanol-assisted growth. Samples were located 0 (I), 4 (II) and 8 (III) cm downstream from the center of the furnace. The temperatures at locations I, II and III were 825˚C, 800˚C and 775˚C, respectively.

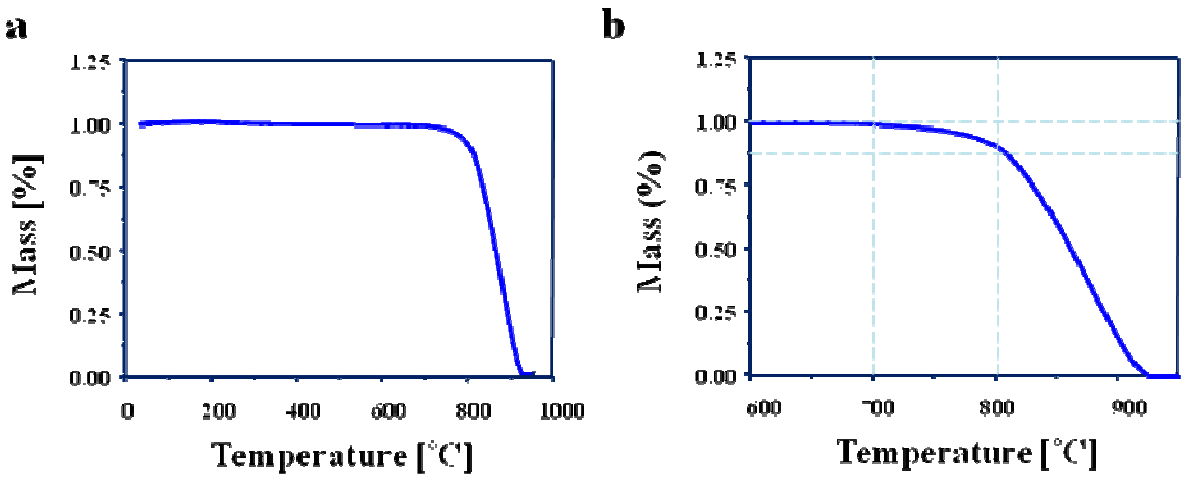

Figure S2. TGA of CNT forest grown with ethanol assistance at 825˚C: (a) Mass as a function of oxidation temperature, with (b) showing the region from 600 to 950˚C. The CNT growth time was 40 minutes and the forest is about 3 mm high.

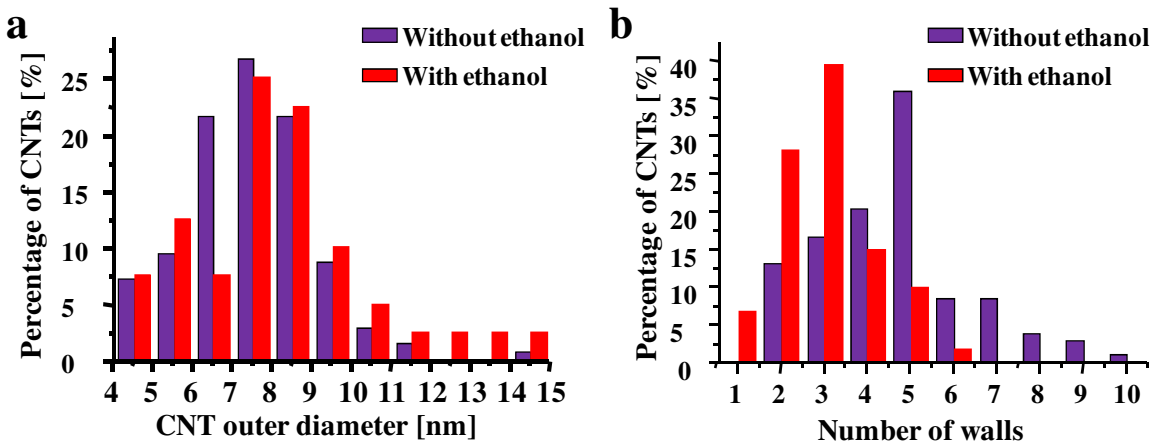

Figure S3. Diameter and wall number statistics of CNTs grown with and without ethanol, measured from TEM images. (a) Diameter distributions of the CNTs grown with (red bars) and without (purple bars) ethanol. (b) The number of walls distributions of the CNTs grown with (red bars) and without (purple bars) ethanol. The average diameters of the CNTs with (61 tubes) and without (139 tubes) ethanol are approximately 8.1 and 8.5 nm, respectively. The average number of walls of the CNTs with (61 tubes) and without (109 tubes) ethanol are 3.0 and 4.6 nm, respectively. The CNTs grown with and without ethanol were synthesized at 825˚C from 1 nm Fe/10 nm Al_2O_3 catalyst film, with 100 sccm He bubbled through ethanol at room temperature.

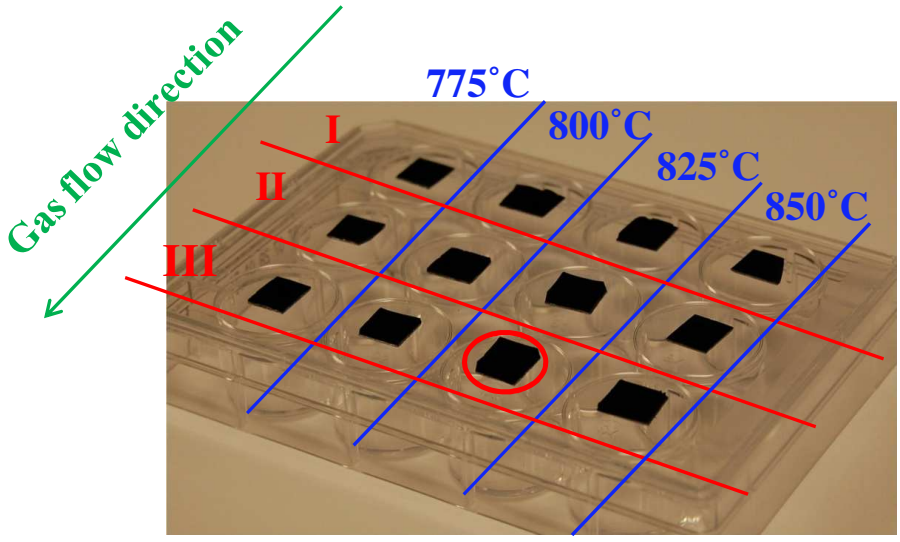

Figure S4. Optical images of CNT forests grown at different furnace setpoint temperatures and locations along the furnace tube. In each experiment, three samples were put at three locations which were (I) 0 cm, (ii) 4 cm, and (III) 8 cm away from the middle of the furnace. The tallest and most uniform forest was obtained at location III, when the furnace was set at 825˚C, representing a sample temperature of 775˚C.

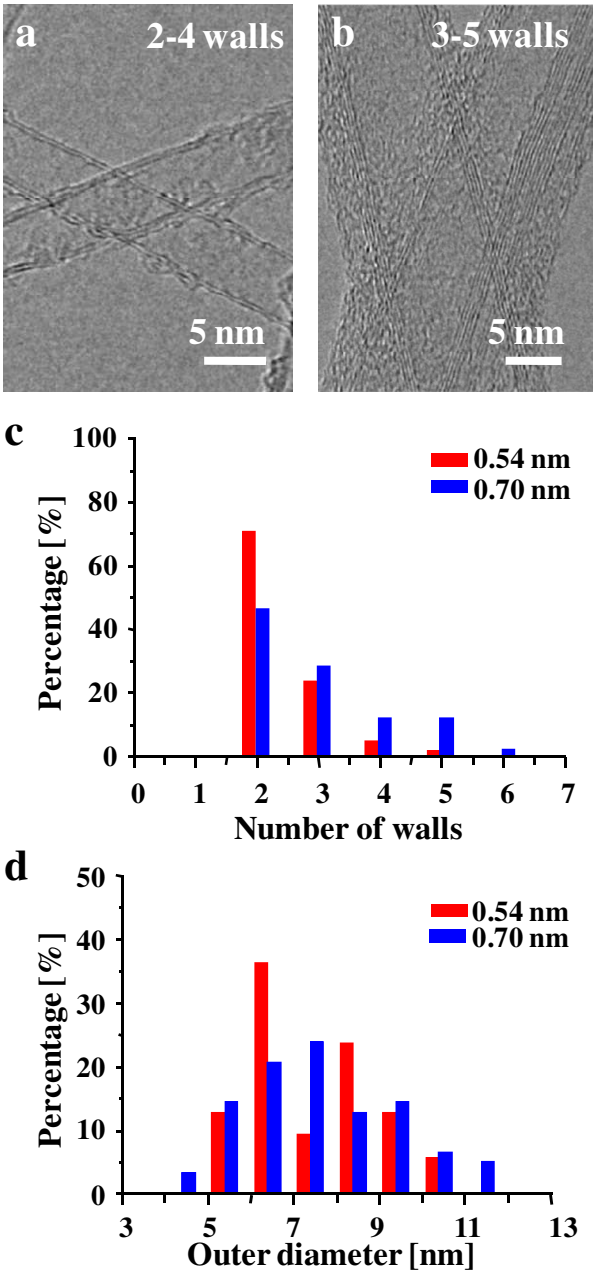

Figure S5. Effect of Fe thickness on the wall number and diameter of CNTs grown by the ethanol-assisted method: (a, b) Typical TEM images of the CNTs grown from 0.54 and 0.70 nm Fe films, respectively. (c) Wall number statistics grown from 0.54 and 0.70 nm Fe films, sampled from the respective locations in the forest shown in Fig. 6. (d) Wall number statistics grown from 0.54 and 0.70 nm Fe films, sampled from the respective locations in the forest shown in Fig. 6. The average diameters of the CNTs from the 0.54 and 0.70 nm Fe regions are 7.0 nm (64 CNTs) and 7.2 nm (50 CNTs) correspondingly.

1. Gregoire, J.M., et al., *Getter sputtering system for high-throughput fabrication of composition spreads.* Review of Scientific Instruments, 2007. **78**(7).
2. Gregoire, J.M., et al., *Resputtering phenomena and determination of composition in codeposited films.* Physical Review B, 2007. **76**(19).